& Gaudreau, 1974), est en effet constituée de chaînes cette fois linéaires et parallèles de dodécaèdres $[ZrF_8]^{4-}$ reliés par des arêtes successivement verticales et horizontales.

Conclusion

La détermination de la structure de la variété α de BaZrF$_6$ nous a permis de mettre en évidence l'existence d'un ion complexe dinucléaire $[Zr_2F_{12}]^{4-}$, d'un type inédit à notre connaissance, mais que nous avons pu comparer aux polyèdres $[Zr_2F_{12}]^{4-}$ de $K_2Cu(ZrF_6)_2.6H_2O$ et $[Zr_2F_{14}]^{6-}$ de $Cu_3Zr_2F_{14}.16H_2O$ d'une part, et au polyèdre $[Zr_2F_{13}]^{5-}$ de $Na_5Zr_2F_{13}$ d'autre part.

Cette structure, comme celle de PbZrF$_6$ déjà déterminée, s'inscrit parfaitement bien dans le cadre général des composés fluorés déjà connus du zirconium. Elles illustrent une fois de plus le caractère cristallochimique particulier du zirconium. Cet élément, combiné en particulier avec le fluor et les éléments alcalins ou alcalino-terreux de taille élevée, tend à former des composés définis de type ionique où il s'associe au fluor de manière très souple en polyèdres de coordinence variée (6, 7 ou 8). Ces polyèdres ont fortement tendance à s'associer entre eux par des ponts fluorés pour donner, soit des ions polynucléaires comme $[Zr_2F_{12}]^{4-}$ dans BaZrF$_6$ α, ou encore $[Zr_2F_{13}]^{5-}$, $[Zr_2F_{14}]^{6-}$ et $[Zr_6F_{31}]^{7-}$ (Burns, Ellison & Levy, 1968), soit des chaînes infinies comme dans PbZrF$_6$ et BaZrF$_6$ β. Les ions alcalins ou alcalino-terreux s'intercalent entre les ions complexes ou les chaînes, assurant la stabilité de l'ensemble.

Références

Burns, J. H., Ellison, R. D. & Levy, H. A. (1968). *Acta Cryst.* B**24**, 230–237.

Fischer, J. & Weiss, R. (1973). *Acta Cryst.* B**29**, 1958–1962.

Herak, R. M., Malčić, S. S. & Manojlović, Lj. M. (1965). *Acta Cryst.* **18**, 520–522.

International Tables for X-ray Crystallography (1968). Vol. III, 2^e éd., pp. 215–216. Birmingham: Kynoch Press.

Laval, J. P., Mercurio-Lavaud, D. & Gaudreau, B. (1974). *Rev. Chim. Minér.* **11**, 742–750.

McDermott, T. E. (1973). *Coord. Chem. Rev.* **11**, 1–20.

McMaster, W. H., Kerr del Grande, N., Mallet, J. H. & Hubbel, J. H. (1969). *Compilation of X-ray Cross Sections*, Natl Bur. Stand. UCRL-50174, Sec. II, Rev. 1.

Mehlhorn, B. & Hoppe, R. (1976). *Z. Anorg. Allg. Chem.* **425**, 180–188.

Penneman, R. A., Ryan, R. R. & Rosenzweig, A. (1973). *Struct. Bonding (Berlin)*, **13**, 1–52.

Acta Cryst. (1978). B**34**, 1074–1079

The Crystal Structures of the ThSiO$_4$ Polymorphs: Huttonite and Thorite

By Mark Taylor

Department of Geology, Stanford University, Stanford, CA 94305, *USA*

and R. C. Ewing

Department of Geology, University of New Mexico, Albuquerque, NM 87131, *USA*

(*Received* 22 *December* 1976; *accepted* 19 *October* 1977)

The structures of the ThSiO$_4$ polymorphs, huttonite and thorite, have been redetermined by single-crystal X-ray diffraction techniques. Huttonite is monoclinic, space group $P2_1/n$, with $a = 6{\cdot}784 \pm 0{\cdot}002$, $b = 6{\cdot}974 \pm 0{\cdot}003$, $c = 6{\cdot}500 \pm 0{\cdot}003$ Å, $\beta = 104{\cdot}92 \pm 0{\cdot}03°$, and $Z = 4$. Thorite is tetragonal, space group $I4_1/amd$, with $a = b = 7{\cdot}1328 \pm 0{\cdot}0002$, $c = 6{\cdot}3188 \pm 0{\cdot}0002$ Å, and $Z = 4$. Both structures were solved by the heavy-atom method and refined by full-matrix least squares to weighted residuals of 0·056 and 0·062 respectively. Huttonite is confirmed to be isostructural with monazite, consisting of SiO$_4$ monomers and a compact arrangement of edge-sharing ThO$_9$ polyhedra. Thorite is isostructural with zircon, consisting of SiO$_4$ monomers and a relatively open arrangement of edge-sharing ThO$_8$ polyhedra. Structural features which might contribute to the difference in radiation-damage susceptibility between these two phases are discussed.

Introduction

Thorite and huttonite are the two known phases of ThSiO$_4$. Both phases occur naturally, but show markedly different behavior toward metamictization – the process of a solid changing from the crystalline to amorphous state in the presence of fissionable nuclides (Graham & Thornber, 1974; Ewing, 1975). Thorite is often found as euhedral tetragonal grains which are partially or fully metamict while huttonite has been found only in the crystalline state. Since thorite and huttonite are isochemical, they receive about the same radiation flux and provide models for examination of structural controls on metamictization. The objective of this study is to provide precise structural details of these two phases.

While not a common mineral, thorite is a well known accessory in pegmatites and schists. It is isostructural with zircon ($ZrSiO_4$) and has been examined on two occasions using powder techniques (Fuchs & Gebert, 1958; Sinha & Prasad, 1973). While these examinations gave consistent results, we felt that the observed Si—O bond lengths (1·54 Å) were anomalously short and that the thorite structure merited a single-crystal refinement. Huttonite is quite rare and was identified as a unique phase of $ThSiO_4$ by Pabst & Hutton (1951). Pabst suggested that huttonite should be isostructural with monazite, $CePO_4$, based on the cell content, cell parameters, and space group, though no previous single-crystal work has confirmed this.

Crystal structure of huttonite

Experimental

While natural samples of huttonite and thorite are available, we felt that a structure determination required pure synthetic material of known thermal history. Huttonite crystals were grown in 5 mm Pt tubes from a Na_2WO_4 melt which was 10% by weight $ThO_2.SiO_2$ (ThO_2 from K & K Laboratories; amorphous SiO_2 from Amersil). The charge was held at 1250°C for two days in an air-atmosphere muffle furnace. This technique is similar to that of Finch, Harris & Clark (1964). The small euhedral crystals (up to 0·3 mm) were easily separated from the flux by boiling in water. Electron-microprobe scans of the crystal showed only traces of Na and W.

Intensity data were collected on a prismatic crystal (0·04 × 0·04 × 0·07 mm) mounted with the c axis parallel to the φ axis of the goniometer. Data were collected automatically on a Picker FACS-1 system using graphite-monochromatized Mo $K\alpha$ radiation. Cell parameters were refined by least-squares analysis of the setting angles from 12 automatically centered reflections in the 2θ range 41·19 to 50·79°. Intensity data were collected from one quadrant of reciprocal space to a maximum $\sin\theta/\lambda$ of 0·807 Å^{-1} using a θ–2θ scan, a scan rate of 1° min^{-1}, and a scan width of 2·0° plus the α_1–α_2 dispersion. Backgrounds were estimated from 10 s counts at both ends of the scan. Standard deviations were estimated using the formula of Corfield, Doedens & Ibers (1967) with an instrumental instability constant of 0·04. Of the 1312 unique reflections collected, 872 had intensities greater than $3\sigma(I)$. All others were considered unobserved and were not used in the subsequent analysis. Data were corrected for Lorentz and polarization effects assuming a 50% ideally crystalline monochromator. Absorption corrections were performed using the analytical technique described by de Meulenaer & Tompa (1965).* Maximum and minimum transmission coefficients were 0·141 and 0·067 respectively.

Crystal data

Huttonite is monoclinic with systematic extinctions $h0l$: $h + l = 2n + 1$; and $0k0$: $k = 2n + 1$. The only space group consistent with these extinctions is $P2_1/n$. Cell parameters are: $a = 6{\cdot}784 \pm 0{\cdot}002$, $b = 6{\cdot}974 \pm 0{\cdot}003$, $c = 6{\cdot}500 \pm 0{\cdot}003$ Å, $\beta = 104{\cdot}92 \pm 0{\cdot}03°$, $V = 297{\cdot}14$ Å^3. There are four formula units per unit cell giving a calculated density of 7·25 g cm^{-3}. This compares with the pycnometer-determined density of 7·20 ± 0·1 g cm^{-3} (Finch *et al.*, 1964). The linear absorption coefficient for Mo $K\alpha$ radiation is 722·8 cm^{-1}. All atoms are on general positions.

Structure determination

The huttonite structure was solved by the heavy-atom method. The Th position was deduced from the F^2 (Patterson) synthesis and the Si position was determined from an F_{obs} synthesis using signs calculated from the Th position. The scale factor was then refined in two cycles of least squares and a subsequent difference synthesis revealed the positions of all four O atoms, though a number of large ripples around the Th position complicated the map. All calculations used the un-ionized coherent scattering factors of Cromer & Mann (1968) and the anomalous-scattering factors of Cromer & Liberman (1970).

The least-squares refinement of the structure converged to a maximum shift/error of 0·08 after four cycles with all isotropic thermal parameters and four cycles with anisotropic Th thermal parameters. One scale factor and a secondary-extinction factor were also varied. Weights were assigned as $[1/\sigma(F)]^2$. The weighted residual, $R_w = [\Sigma\, w(\Delta F)^2/\Sigma\, w(F_{\text{obs}})^2]^{1/2}$, was 0·056 and the conventional residual, $R = \Sigma\,||F_{\text{obs}}| - |F_{\text{calc}}||/\Sigma\,|F_{\text{obs}}|$, was 0·051. The standard deviation of an observation of unit weight was 1·44. When reflections which had been considered unobserved were included, R_w was 0·070. Additional attempts to refine

---

* The computer programs used in this study were: *AGNOST*, an absorption correction program originally written by Coppens, Leiserowitz & Rabinovich; *FORDAP*, A. Zalkin's Fourier synthesis program; *RFINE* and *ERROR*, L. Finger's least-squares and function and error programs; *ORTEP*, C. Johnson's structure plotting program; and unpublished programs by K. Keefer.

the anisotropic thermal parameters of the Si and O atoms did not improve the model at the 0·005 significance level (Hamilton, 1965). Two strong, low-angle reflections, 200 and 120, were apparently affected by extinction, but they were included in the data set. A final difference Fourier synthesis showed no significant detail.

Compilations of F_{obs}, F_{calc}, and the associated $\sigma(F)$ for both the huttonite and thorite structure analyses are given in Table 1;* fractional coordinates and thermal parameters in Table 2; and selected bond lengths and angles in Tables 3 and 4 respectively.

Structure description

The huttonite structure consists of a three-dimensional network of edge-sharing Th polyhedra which are interconnected by SiO_4 tetrahedral monomers (Fig. 1*a*). Each Th atom is coordinated by four *axial* O atoms (denoted by primes in Fig. 2*a*) and five *equatorial* O atoms, for a total coordination number of nine. The axial O atoms represent two edges on opposite sides of the ThO_9 polyhedron shared with SiO_4 groups forming chains parallel to **c** (Fig. 3*a*). The equatorial O atoms represent polyhedral corners shared between the ThO_9 and SiO_4 groups, and they form a nearly planar pentagonal array around Th in a plane perpendicular to **c**. Th–O bond lengths range from 2·43 to 2·81 Å for the axial O atoms and 2·40 to 2·58 Å for the equatorial O atoms. O(2), O(3), and O(4) are each coordinated by one Si and two Th atoms (one axial and one equatorial Th–O bond). O(1) is coordinated by one Si and three Th atoms (one axial and two equatorial Th–O bonds). The increased coordination of O(1) is reflected in its longer bonds to Th.

Table 2. *Positional and thermal parameters*

The quoted anisotropic temperature factor ($\times 10^4$) is $\exp[-(\Sigma_i \Sigma_j h_i h_j \beta_{ij})]$. B_{iso} is the isotropic temperature factor, or, for anisotropic atoms, the equivalent isotropic temperature factor $\frac{4}{3}(\Sigma_i \Sigma_j g_{ij} \beta_{ij})$, where the g_{ij} are elements of the real-space metric tensor. Estimated standard errors are shown in parentheses.

	x	y	z	B_{iso} (Å^2)
Huttonite				
Th	0·2828 (1)	0·1550 (1)	0·0988 (1)	0·37 (1)*
Si	0·3020 (6)	0·1616 (7)	0·6117 (7)	0·46 (6)
O(1)	0·3900 (17)	0·3388 (18)	0·4967 (19)	0·55 (16)
O(2)	0·4803 (18)	0·1060 (16)	0·8234 (18)	0·49 (19)
O(3)	0·1216 (19)	0·2122 (18)	0·7245 (20)	0·55 (17)
O(4)	0·2451 (19)	0·4976 (19)	0·0626 (20)	0·85 (21)
Thorite				
Th	0·0	0·75	0·125	0·30 (3)†
Si	0·0	0·75	0·625	0·55 (1)
O	0·0	0·0732 (13)	0·2104 (16)	0·59 (10)

* $\beta_{11} = 29$ (1), $\beta_{22} = 16$ (1), $\beta_{33} = 18$ (1), $\beta_{12} = -1$ (1), $\beta_{13} = 6$ (1), $\beta_{23} = 3$ (1).

† $\beta_{11} = 16$ (1), $\beta_{22} = 16$ (1), $\beta_{33} = 15$ (2), $\beta_{12} = \beta_{13} = \beta_{23} = 0$.

Table 3. *Interatomic distances* (Å)

Huttonite		Thorite	
Axial Th–O			
Th–O(1)′	2·81 (1)	4 Th–O′	2·47 (1)
Th–O(2)′	2·52 (1)		
Th–O(3)′	2·43 (1)		
Th–O(4)′	2·51 (1)		
Equatorial Th–O			
Th–O(1)	2·58 (1)	4 Th–O	2·37 (1)
Th–O(1)	2·50 (1)		
Th–O(2)	2·40 (1)		
Th–O(3)	2·41 (1)		
Th–O(4)	2·41 (1)		
SiO_4 tetrahedron			
Si–O(1)	1·64 (1)	4 Si–O	1·63 (1)
Si–O(2)	1·63 (1)		
Si–O(3)	1·62 (1)		
Si–O(4)	1·58 (1)		

Table 4. *Selected interatomic angles* (°) *with estimated standard errors in parentheses* (*primes refer to Fig.* 2)

Huttonite		Thorite	
Axial O–Th–O			
O(3)′–Th–O(2)′	59·7 (4)	2 O′–Th–O′	61·5 (5)
O(1)′–Th–O(4)′	56·8 (4)		
Equatorial O–Th–O			
O(4)–Th–O(1)	83·2 (4)	4 O–Th–O	93·0 (1)
O(1)–Th–O(1)	63·1 (5)		
O(1)–Th–O(2)	68·2 (4)		
O(2)–Th–O(3)	72·1 (4)		
O(3)–Th–O(4)	73·8 (5)		
Shared-edge O–Si–O			
O(1)′–Si–O(4)′	104·4 (7)	2 O′–Si–O′	101·0 (7)
O(2)′–Si–O(3)′	98·8 (7)		
Unshared-edge O–Si–O			
O(1)–Si–O(2)	106·7 (6)	4 O–Si–O	113·9 (4)
O(1)–Si–O(3)	116·7 (7)		
O(2)–Si–O(4)	113·7 (7)		
O(3)–Si–O(4)	116·4 (7)		
c-axis chain kink			
Si–Th–Si	175·3 (2)	Si–Th–Si	180·0

---

* Table 1 has been deposited with the British Library Lending Division as Supplementary Publication No. SUP 33204 (9 pp.). Copies may be obtained through The Executive Secretary, International Union of Crystallography, 13 White Friars, Chester CH1 1NZ, England.

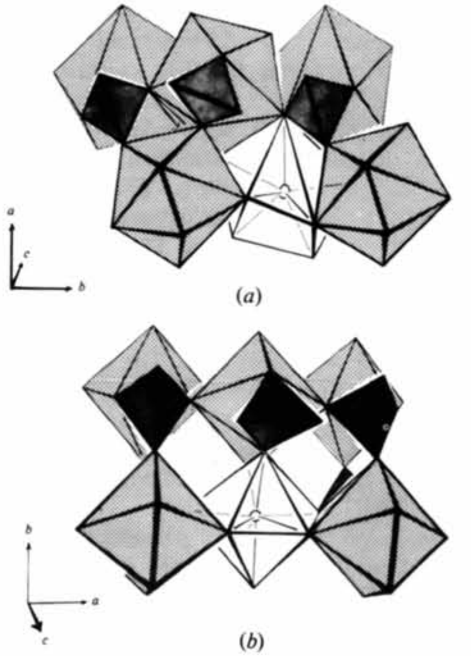

(a)

(b)

Fig. 1. Perspective polyhedral representation of the (a) huttonite, and (b) thorite structures. Darker tetrahedra are SiO_4 groups and lighter polyhedra are (a) ThO_9 and (b) ThO_8 groups.

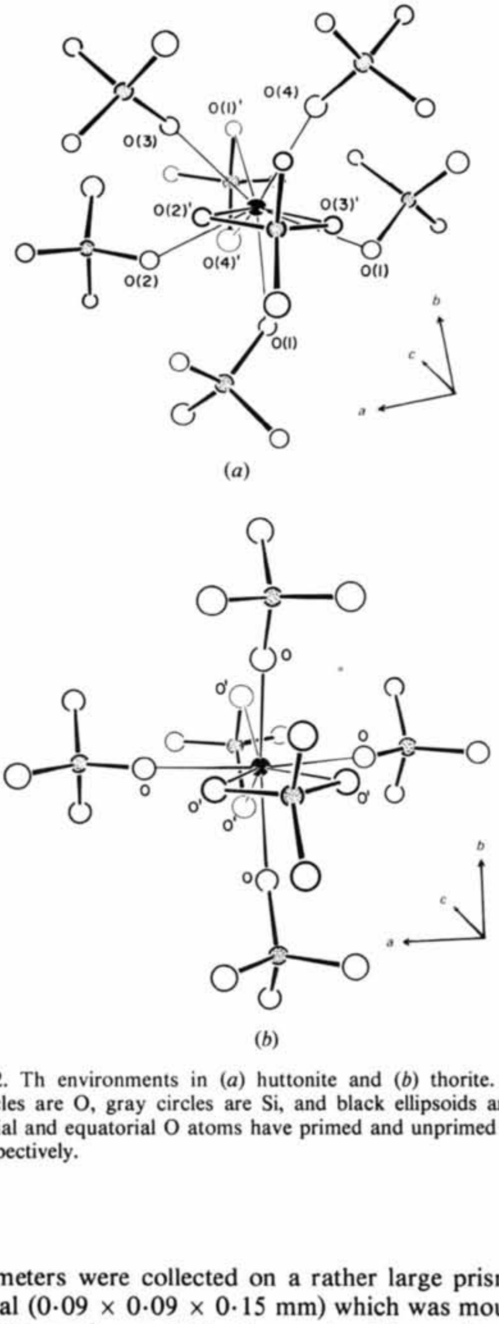

(a)

(b)

Fig. 2. Th environments in (a) huttonite and (b) thorite. Open circles are O, gray circles are Si, and black ellipsoids are Th. Axial and equatorial O atoms have primed and unprimed labels respectively.

Monazite (monoclinic $CePO_4$) is isostructural with huttonite, but a careful comparison is not possible because of discrepancies among the three most recent studies of the monazite structure (Mooney-Slater, 1962; Ghouse, 1965; Ueda, 1967). All three studies show chains parallel to **c**, like those found in huttonite (Fig. 3a), but the Ce—O bond lengths differ by as much as 0·35 Å and the coordination about Ce is different in each case. The structure given by Mooney-Slater (1962) is probably closest to the huttonite structure determined in this study. She reports an eightfold Ce coordination, but if her unlisted Ce—O(2) distance of 2·75 Å is taken in the first coordination sphere, the Ce site is nearly identical in shape to the Th site in huttonite. The average equatorial Th—O length in huttonite (2·46 Å) is quite close to that derived from the monazite structure (2·45 Å) reported by Mooney-Slater, but the average axial Th—O length in huttonite (2·56 Å) is somewhat shorter than that for monazite (2·66 Å).

Crystal structure of thorite

Experimental

Thorite crystals were grown at 1100°C using the same procedure described for huttonite. Due to problems with cleavage, intensity data and cell parameters were collected on a rather large prismatic crystal (0·09 × 0·09 × 0·15 mm) which was mounted with the c axis parallel to the φ axis of the goniometer. Conditions for data collection were the same as described for huttonite, with the following exceptions: twelve reflections used in the cell-parameter determination were in the 2θ range 60·87 to 68·89°; intensity data were collected to a maximum $\sin\theta/\lambda$ of 0·857 $Å^{-1}$ in one octant of reciprocal space; and backgrounds were measured for 20 s. The absorption corrections gave maximum and minimum transmission factors of 0·078 and 0·019. Of 466 space-group reflections initially collected, there were 223 symmetry-equivalent pairs. The intensities for these reflections

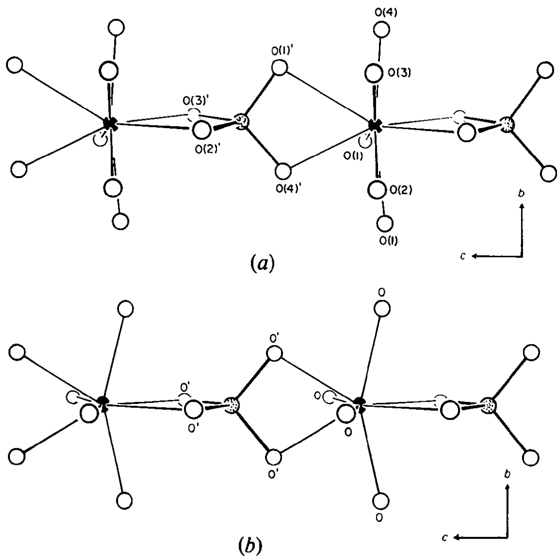

Fig. 3. The c-axis chains in (a) huttonite and (b) thorite.

were averaged and their standard deviations were estimated as:

$$\sigma(I)_{\text{ave}} = \left[\frac{1}{\sum(1/\sigma_i)^2} + (pI_{\text{ave}})^2\right]^{1/2}$$

where σ_i are the individual estimated standard deviations due to counting statistics only and p is the instrument instability constant. The unique data set consisted of 244 reflections, of which 211 had intensities greater than $3\sigma(I)$ and were used in the subsequent refinement.

Crystal data

Thorite is tetragonal with systematic extinctions hkl: $h + k + l = 2n + 1$; $hk0$: $h = 2n + 1$; hhl: $2h + l = 4n$. The only space group consistent with these extinctions is $I4_1/amd$. Cell parameters are: $a = b = 7{\cdot}1328 \pm 0{\cdot}0002$, $c = 6{\cdot}3188 \pm 0{\cdot}0002$ Å, $V = 321{\cdot}48$ Å^3. There are four formula units per unit cell. The calculated density is 6·70, compared with 6·63 ± 0·1 g cm^{-3} determined by pycnometer (Finch *et al.*, 1964). The linear absorption coefficient is 664·2 cm^{-1}.

Structure determination

Thorite has the zircon structure and the only positional variables are the y and z coordinates of O. The cell has been chosen such that the center of symmetry is at the origin and the quoted atom positions are consistent with those of Robinson, Gibbs & Ribbe (1971) in their refinement of the zircon structure. Two cycles of least squares were calculated in which the isotropic thermal parameters for Th and Si were varied. A subsequent F_{obs} synthesis showed the O position. Three additional cycles of refinement with isotropic thermal parameters and six with anisotropic thermal parameters for Th led to a maximum shift/error of 0·03 and a weighted residual of 0·066. While approximately ten strong, low-angle reflections fit the final model rather poorly, three reflections, 332, 220, and 112, showed $F_{\text{calc}} \gg F_{\text{obs}}$, indicating extinction effects or poor corrections for absorption. These three reflections were excluded from the final cycles of refinement yielding a final weighted residual of 0·062, a conventional residual of 0·048, and a standard deviation of a reflection of unit weight of 2·82. The weighted residual for all space-group reflections was 0·072. Attempts to refine the anisotropic thermal parameters of Si and O did not produce a significant improvement in the residual, and a final difference synthesis showed no significant detail.

Positional and thermal parameters and their estimated standard deviations are shown in Table 2; and selected interatomic distances and angles are compared with those of huttonite in Tables 3 and 4 respectively. As in the huttonite structure, the standard errors on the O positions are rather large due to the dominance of the Th contribution to the total scattering.

Structure description

The thorite structure is illustrated in Fig. 1(b). The Th atom is coordinated by four axial and four equatorial O atoms for a total coordination number of eight. The axial O atoms (denoted by primes in Fig. 2b) are bonded to Th and Si such that SiO_4 shares opposite edges with the ThO_8 group forming chains parallel to **c**, identical to those in huttonite (Fig. 3b). The axial Th–O bonds are all 2·47 Å. The four equatorial O atoms form a flattened tetrahedral array around Th and all have a Th–O bond length of 2·36 Å. Each O is coordinated by one Si, one Th in the axial position, and one Th in the equatorial position. A detailed description of the zircon/thorite structure type is presented by Robinson *et al.* (1971).

Discussion

Due to the difficulty in reversing the phase transition, the true thermodynamic relationship of thorite and huttonite is not clear, and their relative stabilities are difficult to assess. Mumpton & Roy (1961) have suggested that thorite is metastable at all temperatures and its prevalence in nature is due to crystal-growth kinetics. However, thorite is usually taken to be the low-temperature polymorph (Finch *et al.*, 1964) with the transition occurring around 1225 °C. This means that with increasing temperature, $ThSiO_4$ must change from the low-density, high-symmetry thorite phase to the higher-density, lower-symmetry huttonite phase, in contrast to the usual trends. On the other hand, the volume of the Th polyhedron (the vertices being defined by the nearest-neighbor O atoms) is 25·2 Å^3 for thorite and 30·4 Å^3 for huttonite, suggesting an expansion of the Th site with higher temperatures.

Stability criteria based on radius ratio and charge balance are inconclusive; the Th/O radius ratio (0·76) suggests that the ninefold coordinated huttonite structure should be preferred, while a calculation of Pauling charge balance (Pauling, 1960) indicates that O(1) of huttonite is overbonded (ζ = 2·5). All O atoms in thorite are exactly charge balanced (ζ = 2·0).

The principal structural difference between thorite and huttonite is the large void space present in thorite (Fig. 2*b*). The voids are centered on fractional coordinates $(\frac{1}{4},\frac{1}{2},\frac{1}{2})$ with an approximately octahedral shape and a volume of 14·0 Å^3. They are interconnected to form channels parallel to **c** and could be responsible for the diffusion of water into the thorite structure. In view of the fact that natural thorites may contain up to 70 mol% water (Hutton, 1950), hydration may play a major role in the metamictization process. A rationalization of the behavior of huttonite and thorite based solely on structure is not possible, and additional experiments examining the role of water and the detailed nature of the metamict state are in progress.

The authors thank A. Pabst for his encouragement and interest during this study, G. E. Brown and K. D. Keefer for a critical reading of the manuscript, and Standard Oil of California for the use of their computer, without which this study would not have been possible. One of us (MT) was supported by NSF Grants GA 41731 and EAR74-03056-A01 during this study.

References

Corfield, R., Doedens, R. J. & Ibers, J. A. (1967). *Inorg. Chem.* **6**, 197–204.

Cromer, D. T. & Liberman, D. (1970). *J. Chem. Phys.* **53**, 1891–1898.

Cromer, D. T. & Mann, J. B. (1968). *Acta Cryst.* A**24**, 321–324.

Ewing, R. C. (1975). *Am. Mineral.* **60**, 728–733.

Finch, C. B., Harris, L. A. & Clark, G. W. (1964). *Am. Mineral.* **49**, 782–785.

Fuchs, L. H. & Gebert, E. (1958). *Am. Mineral.* **43**, 243–248.

Ghouse, K. M. (1965). *Naturwissenschaften*, **52**, 32–33.

Graham, J. & Thornber, M. R. (1974). *Am. Mineral.* **59**, 1047–1050.

Hamilton, W. C. (1965). *Acta Cryst.* **18**, 502–510.

Hutton, C. O. (1950). *Geol. Soc. Am. Bull.* **61**, 635–716.

Meulenaer, J. de & Tompa, H. (1965). *Acta Cryst.* **19**, 1014–1018.

Mooney-Slater, R. C. L. (1962). *Z. Kristallogr.* **117**, 371–385.

Mumpton, F. A. & Roy, R. (1961). *Geochim. Cosmochim. Acta*, **21**, 217–238.

Pabst, A. & Hutton, C. O. (1951). *Am. Mineral.* **36**, 60–69.

Pauling, L. (1960). *The Nature of the Chemical Bond*, 3rd ed., p. 548. Ithaca: Cornell Univ. Press.

Robinson, K., Gibbs, G. V. & Ribbe, P. H. (1971). *Am. Mineral.* **56**, 782–790.

Sinha, D. P. & Prasad, R. (1973). *J. Inorg. Nucl. Chem.* **35**, 2614–2615.

Ueda, T. (1967). *J. Jpn. Assoc. Mineral. Petrol. Econ. Geol.* **58**, 170–179.